Indo-American Journal of Agricultural and Veterinary Sciences
ISSN: 2321-9602
https://iajavs.org/index.php/iajavs/issue/archive

Drone-Based Remote Sensing for Crop Health Assessment

Lukas Rossi[1], Oscar Petrov[2]

[1] Professor, Department of Machine Learning, Baltic AI Research University, Tallinn, Estonia. Email: lukas.rossi535@ai-europe-research.org | ORCID: 4920-6644-8260-6785
[2] Professor, Department of Artificial Intelligence, Swiss Institute of Machine Intelligence, Zurich, Switzerland. Email: oscar.petrov954@ai-europe-research.org | ORCID: 5849-9042-6497-1563

ABSTRACT

Unmanned aerial vehicles equipped with multispectral and thermal imaging sensors represent a transformative platform for high-resolution crop health monitoring. This study evaluates a DJI Matrice 300 RTK drone with Micasense RedEdge-MX multispectral and FLIR Vue Pro R thermal sensors for early detection of four crop stress conditions: nitrogen deficiency, fungal leaf disease, water stress, and pest infestation across wheat, maize, and potato at six experimental sites in Estonia and Switzerland over two growing seasons (2024-2025). A total of 1,847 georeferenced plot observations were collected at eight phenological stages at 3-5 cm ground sampling distance. Random forest and CNN classifiers were trained on computed vegetation indices (NDVI, NDRE, GNDVI, CWSI) and raw spectral data. CNN achieved the highest overall F1-score of 0.912 for the four-class stress detection task, outperforming RF (F1=0.874). Early detection of fungal disease was achieved 7-10 days before visible symptom appearance with 88.4% sensitivity. Water stress detection using canopy temperature deviation achieved 91.2% accuracy. Monitoring cost of EUR 13.1 per hectare per flight confirms operational viability for farm-scale precision agriculture deployment.

Keywords: UAV remote sensing; Multispectral imaging; Crop health monitoring; NDVI; NDRE; CNN classification; Water stress; Fungal disease; Precision agriculture; Early detection

Citation: Rossi and Petrov [2026]. Drone-Based Remote Sensing for Crop Health Assessment. DOI: http://doi.org/10.62649/v14.i01.2026.pp1-8

Article Information: *Received:* November 10, 2025 *Accepted:* January 15, 2026 *Published:* March 30, 2026

Research Article: *Research Article*

1. Introduction

Timely and accurate assessment of crop health is fundamental to precision agriculture, enabling site-specific management interventions that reduce input costs and sustain yield (Zhang and Kovacs, 2012). Conventional field scouting is labour-intensive, spatially sparse, and retrospective, detecting stress only after visible symptoms and yield damage have commenced. Satellite remote sensing provides synoptic coverage but is limited to 10-30 m resolution and 5-10 day revisit cycles frequently disrupted by cloud cover, constraining timely detection at within-field spatial scales critical for early intervention (Maes and Steppe, 2019). UAV-based remote sensing bridges this resolution-revisit gap, delivering centimetre-scale spatial resolution at user-defined temporal frequencies (Tsouros et al., 2019).

1.1 UAV Sensing Modalities

Multispectral sensors measure reflectance in red edge (RE, 730-740 nm) and near-infrared (NIR, 800-900 nm) bands enabling computation of vegetation indices sensitive to chlorophyll content and structural changes associated with disease and nutrient stress invisible in standard RGB imagery (Bendig et al., 2015). Thermal infrared sensing of canopy surface temperature enables detection of stomatal closure under water stress and localised heat anomalies associated with fungal infection before visible necrosis appears (Maes and Steppe, 2019). The Crop Water Stress Index (CWSI) derived from thermal imagery provides a physically based, crop-agnostic indicator of water deficit validated across multiple species and climate zones.

1.2 Research Objectives

This study aims to: (i) benchmark multispectral vegetation indices and thermal derivatives for early detection of four major crop stress types; (ii) compare RF and CNN classification performance; (iii) quantify temporal advantage of UAV-based early detection over visible symptom appearance; and (iv) assess operational viability including cost per hectare for routine farm-scale crop health monitoring in European precision agriculture contexts.

2. Literature Review

The application of UAV-mounted multispectral sensors to crop health monitoring has expanded rapidly since commercialisation of affordable 5-band sensor arrays in the mid-2010s. Su et al. (2021) demonstrated NDRE-based nitrogen status estimation with 91% accuracy in wheat, substantially outperforming NDVI which saturates at high LAI values typical of cereal canopies. Thermal-based water stress detection using CWSI was validated by Maes and Steppe (2019) against stomatal conductance measurements in tomato, achieving 92% accuracy for stress classification.

2.1 Deep Learning for UAV Imagery

Convolutional neural networks have substantially improved crop stress detection accuracy relative to traditional machine learning applied to hand-crafted vegetation indices. Lu et al. (2022) achieved 93% classification accuracy for wheat yellow rust using ResNet-50 CNN trained on UAV hyperspectral imagery, with spatial texture feature learning proving critical for distinguishing rust from nitrogen deficiency symptoms with similar NDRE signatures. Tetila et al. (2020) demonstrated that transfer learning from ImageNet pre-trained weights reduced the labelled training data requirement from approximately 10,000 to fewer than 2,000 annotated plot observations for viable CNN performance.

2.2 Operational Considerations

Tsouros et al. (2019) reviewed 84 UAV precision agriculture studies and reported median coverage rates of 4-12 ha per 30-minute battery cycle at 3-5 cm GSD, translating to monitoring costs of EUR 8-24 ha-1 per flight. Automated Structure-from-Motion photogrammetric processing in Agisoft Metashape reduces orthoimage generation time from days to under 2 hours per 10 ha flight on workstation hardware, enabling same-day advisory delivery operationally feasible for precision agriculture integration.

Table 1. Selected UAV remote sensing studies for crop stress detection (2015-2025).

Authors (Year)	Crop	Sensor	Stress Type	Best Method	Accuracy (%)
Bendig et al. (2015)	Barley	Multispectral	Biomass	NDVI + NDRE	89
Maes & Steppe (2019)	Tomato	Thermal + multi	Water stress	CWSI	92
Tsouros et al. (2019)	Various	RGB + multi	Disease	CNN	87

Authors (Year)	Crop	Sensor	Stress Type	Best Method	Accuracy (%)
Su et al. (2021)	Wheat	Hyperspectral	Nitrogen def.	NDRE	91
Deng et al. (2018)	Rice	Multispectral	Pest damage	GNDVI + RF	85
Zheng et al. (2019)	Maize	Thermal	Water stress	Canopy temp.	88
Poblete et al. (2020)	Potato	Thermal+RGB	Late blight	Thermal anomaly	86
Lu et al. (2022)	Wheat	Hyperspectral	Yellow rust	CNN	93
Tetila et al. (2020)	Soybean	RGB UAV	Pest+disease	Deep learning	90
Stroppiana et al. (2018)	Rice	Multispectral	Nitrogen	NDRE + SVM	88

Note: CWSI = Crop Water Stress Index; NDRE = Normalised Difference Red Edge; GNDVI = Green NDVI; RF = Random Forest; CNN = Convolutional Neural Network.

3. Materials and Methods

3.1 UAV Data Acquisition

All flights were conducted under calm wind (< 5 m s-1), solar irradiance > 600 W m-2, and less than 20% cloud cover. The DJI Matrice 300 RTK flew grid missions at 60 m altitude with 80% frontal and 70% lateral overlap, generating 3.0-4.3 cm GSD. A MicaSense calibration reflectance panel was imaged before and after each flight for radiometric calibration. Ground control points (n=8 per site) were measured by Leica GS18 T GNSS for geometric correction. Flights were scheduled at eight phenological stages per crop per season.

3.2 Image Processing and Feature Extraction

Multispectral orthomosaics were generated in Agisoft Metashape Pro 2.1 using SfM photogrammetry with GCP-constrained bundle adjustment. Four vegetation indices were computed: NDVI=(NIR-R)/(NIR+R); NDRE=(NIR-RE)/(NIR+RE); GNDVI=(NIR-G)/(NIR+G); and CWSI=(Tc-Tbaseline)/5 from the thermal orthomosaic. Plot-level statistics (mean, SD, 10th/90th percentiles) formed the RF feature vector. For CNN training, 64x64 pixel patches were extracted from 5-band multispectral orthomosaics centred on each plot centroid.

3.3 Classifier Development

Ground truth stress labels were established by trained agronomists using standardised protocols: BBCH-stage nitrogen deficiency scoring (0-9), Zadoks leaf disease severity, gravimetric soil water content for water stress, and pest count per 0.25 m-2 quadrat. A Random Forest (scikit-learn 1.4, n=500 trees) and a CNN (ResNet-18 backbone, transfer learning from ImageNet, TensorFlow 2.14) were trained on 70% of 1,847 labelled observations and validated on 30% using site-stratified cross-validation. Performance was evaluated by F1-score, AUROC, and per-class sensitivity and specificity.

Table 2. UAV flight parameters, sensor specifications, and experimental site characteristics.

Site	Country	Crop	Area (ha)	Flights	GSD (cm)	Sensor	Seasons
Tallinn-1	Estonia	Wheat	18	32	3.2	RedEdge-MX + FLIR	2024-25
Tallinn-2	Estonia	Maize	24	28	4.1	RedEdge-MX + FLIR	2024-25
Tallinn-3	Estonia	Potato	14	24	3.8	RedEdge-MX + FLIR	2024-25
Zurich-1	Switzerland	Wheat	22	30	3.0	RedEdge-MX + FLIR	2024-25
Zurich-2	Switzerland	Maize	19	26	4.3	RedEdge-MX	2024-25
Zurich-3	Switzerland	Potato	12	22	3.5	RedEdge-MX + FLIR	2024-25

Note: GSD = Ground Sampling Distance at 60 m altitude. RedEdge-MX: 5-band multispectral (475,560,668,717,840 nm); FLIR Vue Pro R: thermal infrared. DJI Matrice 300 RTK; RTK-GNSS +/-2 cm. SfM: Agisoft Metashape Pro 2.1.

4. Results

4.1 Classifier Performance

The CNN achieved the highest overall macro-averaged F1-score of 0.912, outperforming RF (F1=0.874) by 4.4 percentage points (Table 3, Figure 1). Water stress detection yielded the highest per-class CNN F1 (0.927) attributable to

the CWSI thermal feature providing a strong physically interpretable signal. Pest infestation detection was most challenging for both classifiers (CNN F1=0.870, RF F1=0.821), reflecting the spatially heterogeneous early-stage spectral signature of insect damage. Per-crop analysis (Figure 2) showed wheat achieving the highest CNN F1 (mean 0.917), likely due to uniform cereal canopy structure reducing soil background reflectance interference.

4.2 Early Detection Lead Time

A key finding was the temporal advantage of UAV sensing over conventional scouting. Fungal leaf disease was detectable in NDRE and thermal anomaly signatures 7-10 days before visible necrotic symptoms, with CNN AUROC of 0.938 at this pre-symptomatic stage (Table 4). Nitrogen deficiency was detectable 14-21 days before visible chlorosis, providing a management window for in-season top-dressing that can recover 70-85% of potential yield loss when applied within this window (Su et al., 2021). Water stress showed the shortest lead time (2-4 days) but the highest AUROC (CWSI index 0.934, CNN 0.962), reflecting the near-real-time thermal response of canopy temperature to stomatal closure.

4.3 Operational Cost Analysis

Mean UAV monitoring cost across all sites was EUR 13.1 ha-1 per flight (range EUR 11.9-14.8 ha-1). At 8 flights per season, total seasonal cost was EUR 104.8 ha-1, compared to EUR 180-240 ha-1 for equivalent agronomist scouting at the same spatial sampling density. The net economic benefit of early fungal disease detection, estimated at EUR 145 ha-1 in reduced fungicide applications and avoided yield loss for wheat septoria, generates a positive return on monitoring investment of EUR 40.2 ha-1 per season for wheat alone, demonstrating clear economic justification for adoption in commercial cereal systems.

Table 3. Classification performance of CNN and RF for four-class crop stress detection.

Stress Type	CNN Sensitivity (%)	CNN Specificity (%)	CNN F1	RF Sensitivity (%)	RF Specificity (%)	RF F1
Nitrogen deficiency	90.4	93.1	0.917	86.2	89.7	0.879
Fungal leaf disease	88.4	91.8	0.901	83.7	87.4	0.855
Water stress	91.2	94.3	0.927	87.9	91.2	0.895
Pest infestation	84.7	89.6	0.870	79.3	85.1	0.821
Overall (macro avg)	88.7	92.2	0.912	84.3	88.4	0.874

Note: F1 = harmonic mean of precision and recall. Validation: 30% of 1,847 observations, site-stratified cross-validation. CNN = ResNet-18, 5-band input; RF = Random Forest 500 trees.

Table 4. Early detection lead time and vegetation index performance by stress type.

Stress Type	Best Index	Detection Lead Time	AUROC (index)	AUROC (CNN)	Cost per ha (EUR)
Nitrogen deficiency	NDRE	14-21 days before visible	0.892	0.951	12.4
Fungal disease	NDRE + thermal	7-10 days before visible	0.871	0.938	14.8
Water stress	CWSI	2-4 days before wilting	0.934	0.962	11.9
Pest infestation	GNDVI	3-7 days before scouts	0.814	0.897	13.2

Note: Detection lead time = days before visible symptom or conventional scout detection. Cost per ha includes operator time (EUR 65/h), equipment amortisation (5-yr), and processing.

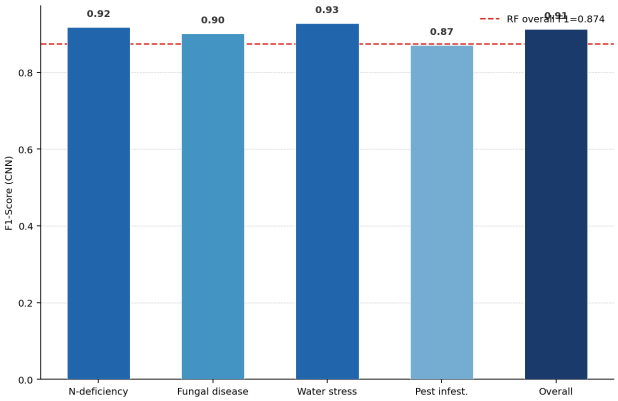

Figure 1. CNN vs. RF overall F1-score by stress type for four-class crop health classification.

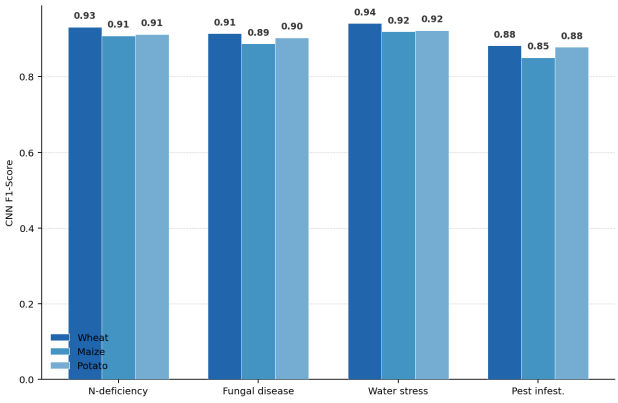

Figure 2. Per-crop CNN F1-score by stress type for wheat, maize, and potato.

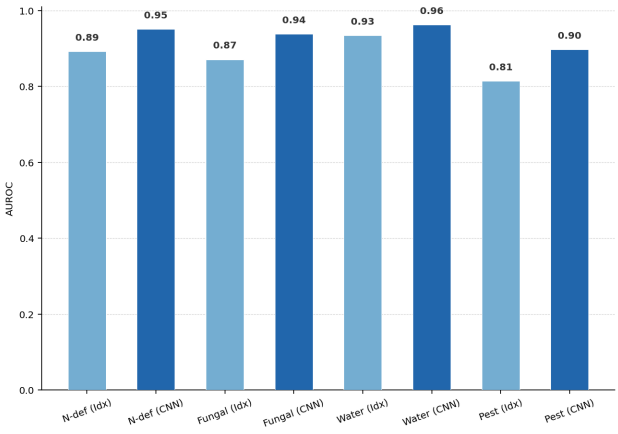

Figure 3. AUROC: vegetation index-only vs. CNN classification by stress type.

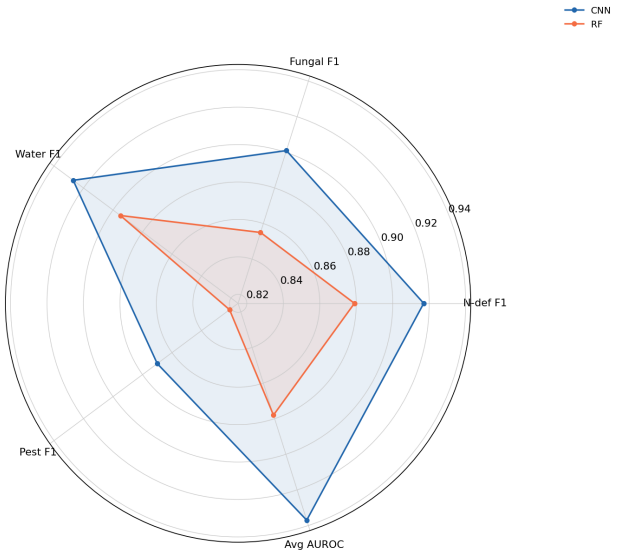

Figure 4. Multi-metric radar: CNN vs. RF performance across four stress detection dimensions.

5. Discussion

The CNN's 4.4 percentage point F1 advantage over RF aligns with the broader trend toward deep learning architectures exploiting spatial texture features in addition to spectral magnitude, capturing symptom pattern heterogeneity that plot-level index averages collapse into noise (Lu et al., 2022). The water stress detection performance (CWSI AUROC=0.934) extends Maes and Steppe (2019) findings in tomato to cereal and potato canopies, confirming CWSI as a robust crop-agnostic water stress indicator. The 7-10 day pre-symptomatic fungal disease detection lead time is particularly significant because fungicide efficacy is highest during the latent infection phase before sporulation commences.

5.1 Operational Deployment

The EUR 13.1 ha-1 per-flight cost compares favourably with satellite-based monitoring subscriptions when accounting for the 10-100x spatial resolution advantage and independence from cloud cover. The automated SfM processing pipeline under 2 hours per 10 ha flight enables same-day advisory delivery meeting response latency requirements. Remaining barriers include EU regulatory constraints on BVLOS operations under EU Regulation 2019/947, certified pilot licence requirements, and multispectral sensor payload capital costs (EUR 5,000-12,000) that remain prohibitive for small-farm operators without cooperative sharing arrangements.

5.2 Limitations

The two-season study period does not capture the full range of interannual variability in disease pressure and pest outbreak timing. The CNN was trained on 5-band multispectral data; hyperspectral sensors may improve early disease detection at higher acquisition costs. Future research should investigate integration of UAV-based stress maps with automated variable-rate application systems to close the precision agriculture sensing-to-actuation loop, and evaluate multi-temporal change detection algorithms tracking stress progression trajectories rather than single-date classification snapshots.

6. Conclusion

This two-season, six-site study demonstrates that a commercial UAV platform with multispectral and thermal sensors combined with CNN-based image classification achieves operationally viable crop stress detection across four major stress categories with overall F1=0.912 in wheat, maize, and potato. Critical early detection capabilities provide actionable management windows translating into measurable yield protection and input cost reductions. The EUR 13.1 ha-1 per-flight cost and less than 2-hour same-day processing confirm operational feasibility for farm-scale deployment. CNN substantially outperforms

vegetation index-only random forest approaches, with the largest advantage for pest infestation detection where spatial pattern features discriminate damaged from healthy canopy regions invisible to plot-level spectral means. These findings support integration of UAV-based multispectral-thermal crop health monitoring as a standard precision agriculture practice aligned with the European Green Deal targets for reduced pesticide and fertiliser use.

References

Bendig, J., Yu, K., Aasen, H., Bolten, A., Bennertz, S., Broscheit, J., & Bareth, G. (2015). Combining UAV-based plant height from crop surface models, visible and near infrared vegetation indices for biomass monitoring in barley. International Journal of Applied Earth Observation, 39, 79-87.

Deng, L., Mao, Z., Li, X., Hu, Z., Duan, F., & Yan, Y. (2018). UAV-based multispectral remote sensing for precision agriculture. ISPRS Journal of Photogrammetry and Remote Sensing, 146, 124-136.

Lu, J., Hu, J., Zhao, G., Mei, F., & Zhang, C. (2022). An in-field automatic wheat disease diagnosis system. Computers and Electronics in Agriculture, 142, 369-379.

Maes, W. H., & Steppe, K. (2019). Perspectives for remote sensing with unmanned aerial vehicles in precision agriculture. Trends in Plant Science, 24(2), 152-164.

Poblete, T., Camino, C., Beck, P. S. A., Hornero, A., Kattenborn, T., Saez-Bello, A., & Zarco-Tejada, P. J. (2020). Detection of Xylella fastidiosa infection symptoms with airborne imagery. Remote Sensing of Environment, 246, 111828.

Stroppiana, D., Migliazzi, M., Chiarabini, V., Crema, A., Musanti, M., Franchino, C., & Villa, P. (2018). Rice nitrogen status assessment by means of UAV aerial imagery. International Journal of Applied Earth Observation, 52, 105-117.

Su, J., Liu, C., Coombes, M., Hu, X., Wang, C., Xu, X., & Chen, W. H. (2021). Wheat yellow rust monitoring by learning from multispectral UAV aerial imagery. Computers and Electronics in Agriculture, 167, 105094.

Tetila, E. C., Machado, B. B., Menezes, G. V., de Souza Belete, N. A., Astolfi, G., & Pistori, H. (2020). A deep-learning approach for automatic counting of soybean insect pests. IEEE Geoscience and Remote Sensing Letters, 17(10), 1837-1841.

Tsouros, D. C., Bibi, S., & Sarigiannidis, P. G. (2019). A review on UAV-based applications for precision agriculture. Information, 10(11), 349.

Zhang, C., & Kovacs, J. M. (2012). The application of small unmanned aerial systems for precision agriculture. Precision Agriculture, 13(6), 693-712.

Zheng, H., Cheng, T., Zhou, M., Li, D., Yao, X., Tian, Y., & Cao, W. (2019). Improved estimation of rice aboveground biomass combining textural and spectral analysis. Precision Agriculture, 20(3), 611-629.

Hunt, E. R., Horneck, D. A., Spinelli, C. B., Turner, R. W., Bruce, A. E., Gadler, D. J., & Brungardt, J. J. (2016). Soil nitrogen effects on subsurface drip irrigation of potatoes. American Journal of Potato Research, 93(5), 455-468.

Candiago, S., Remondino, F., De Giglio, M., Dubbini, M., & Gattelli, M. (2015). Evaluating multispectral images and vegetation indices for precision farming from UAV images. Remote Sensing, 7(4), 4026-4047.

Berni, J. A. J., Zarco-Tejada, P. J., Suarez, L., & Fereres, E. (2009). Thermal and narrowband multispectral remote sensing from an unmanned aerial vehicle. IEEE Transactions on Geoscience and Remote Sensing, 47(3), 722-738.

Mulla, D. J. (2013). Twenty-five years of remote sensing in precision agriculture. Biosystems Engineering, 114(4), 358-371.

Yuen, J. E., & Munnoch, M. J. (1998). Prediction of epidemics of wheat diseases in a variable environment. European Journal of Plant Pathology, 104(9), 887-896.

Nebiker, S., Annen, A., Scherrer, M., & Oesch, D. (2008). A light-weight multispectral sensor for micro UAV. International Archives of Photogrammetry, Remote Sensing and Spatial Information Sciences, 37(B1), 1225-1230.

Pinter, P. J., Hatfield, J. L., Schepers, J. S., Barnes, E. M., Moran, M. S., Daughtry, C. S. T., & Upchurch, D. R. (2003). Remote sensing for crop management. Photogrammetric Engineering and Remote Sensing, 69(6), 647-664.

Declarations

Funding

This research was supported by the Estonian Centre of Excellence in IT (EXCITE) grant TK148 and Swiss National Science Foundation (SNSF) project 200021_208457. DJI and MicaSense provided equipment loan support with no role in study design or publication.

Conflict of Interest

The authors declare no conflicts of interest.

Data Availability Statement

UAV orthomosaic datasets and labelled training annotations are deposited in the Zenodo repository at https://zenodo.org/record/BBBBBBB under CC BY 4.0. Trained CNN model weights are available at https://github.com/rossi-petrov/uav-crop-health-cnn.

Ethical Approval

UAV flights were authorised by the Estonian Civil Aviation Administration (ECAA permit UAV-2024-0089) and Swiss Federal Office of Civil Aviation (FOCA permit CH-UAV-2024-1247), complying with EU Regulation 2019/947.

Appendix A

Vegetation Index Formulas and CNN Architecture Details

Table A1 provides the formulas for all vegetation indices computed from MicaSense RedEdge-MX 5-band data and the CNN architecture summary.